arXiv:1605.06357v1 [quant-ph] 20 May 2016

Physical origins of ruled surfaces on the reduced density matrices geometry

Ji-Yao Chen,[1,2] Zhengfeng Ji,[3,4] Zheng-Xin Liu,[5] Xiaofei Qi,[6] Nengkun Yu,[7,3,8] Bei Zeng,[8,7] and Duanlu Zhou[9]

[1]*State Key Laboratory of Low Dimensional Quantum Physics, Department of Physics, Tsinghua University, Beijing, China*
[2]*Perimeter Institute for Theoretical Physics, Waterloo, Ontario, Canada*
[3]*Centre for Quantum Computation & Intelligent Systems, School of Software, Faculty of Engineering and Information Technology, University of Technology Sydney, Sydney, Australia*
[4]*State Key Laboratory of Computer Science, Institute of Software, Chinese Academy of Sciences, Beijing, China*
[5]*Department of Physics, Renmin University of China, Beijing, China*
[6]*Department of Mathematics, Shanxi University, Taiyuan, Shanxi, China*
[7]*Institute for Quantum Computing, University of Waterloo, Waterloo, Ontario, Canada*
[8]*Department of Mathematics & Statistics, University of Guelph, Guelph, Ontario, Canada*
[9]*Institute of Physics, Chinese Academy of Sciences, Beijing, China*

(Dated: March 8, 2022)

The reduced density matrices (RDMs) of many-body quantum states form a convex set. The boundary of low dimensional projections of this convex set may exhibit nontrivial geometry such as ruled surfaces. In this paper, we study the physical origins of these ruled surfaces for bosonic systems. The emergence of ruled surfaces was recently proposed as signatures of symmetry-breaking phase. We show that, apart from being signatures of symmetry-breaking, ruled surfaces can also be the consequence of gapless quantum systems by demonstrating an explicit example in terms of a two-mode Ising model. Our analysis was largely simplified by the quantum de Finetti's theorem—in the limit of large system size, these RDMs are the convex set of all the symmetric separable states. To distinguish ruled surfaces originated from gapless systems from those caused by symmetry-breaking, we propose to use the finite size scaling method for the corresponding geometry. This method is then applied to the two-mode XY model, successfully identifying a ruled surface as the consequence of gapless systems.

PACS numbers: 03.65.Wj, 03.65.Ud, 03.67.Mn

I. INTRODUCTION

Natural interactions in a many-body system usually involve only a few particles. For an N-particle system, the Hamiltonian of the system adopts the form $H = \sum_j H_j$ with each H_j acting nontrivially on, in most cases, only two particles. For any quantum state $|\psi^N\rangle$ of the system, its energy can then be determined by its two-particle reduced density matrices (2-RDMs). Consequently, the ground state energy of the system can be solely read out from the 2-RDMs of the ground state $|\psi_0^N\rangle$.

For a Hamiltonian $H(\vec{\lambda})$ containing some set of parameters $\vec{\lambda}$, the ground state $|\psi_0^N(\vec{\lambda})\rangle$ may change suddenly while the parameter $\vec{\lambda}$ changes smoothly, leading to a quantum phase transition. Such a change can also be captured by the 2-RDMs of $|\psi_0^N(\vec{\lambda})\rangle$, which is reflected by a sudden change in the set of all the 2-RDMs, which is known to be convex. It is then highly desired to characterize such changes geometrically on the set of 2-RDMs.

However, the geometric shape of the set of 2-RDMs, denoted by Θ_2^N, is notoriously hard to characterize in general, apart from the obvious fact that Θ_2^N is a convex set. How to characterize Θ_2^N has been a central topic of research in the quantum marginal problem and the N-representability problem, which dates back to the 1960s [1–5]. Recently, it has been shown that the characterization of Θ_2^N is a hard problem even with the existence of a quantum computer [6–8]. Nevertheless, many practical approaches are developed to characterize the properties of the set, and to retrieve useful information that characterizes the physical properties of the system [9, 10].

Among these approaches, one important idea is to study the 2 and 3 dimensional projections of these 2-RDMs [4, 5, 9, 10], such that the properties of the different quantum phases are visually available. It has been shown that a flat portion of the 2-dimensional projection can already signal first-order phase transitions [11, 12]. However, for continuous phase transitions, 2-dimensional projections contain no information, and one needs to further examine 3-dimensional projections.

It is observed that the emergence of ruled surfaces on the boundary of the 3-dimensional projections of the 2-RDMs signatures symmetry-breaking phase [12]. With a generalization, the ruled surfaces can also signal the symmetry protected topological phase [13]. And it is interesting to note that the connection of ruled surfaces on the boundary of certain convex body and phase transitions dates back to Gibbs in the 1870's [14–17]. The convex bodies under consideration in Gibbs' original work are in the context of classical thermodynamics, and the case of quantum many-body physics is rather different. It nevertheless indicates that the convex geometry approach is a fundamental and universal idea.

It remains unclear whether there are other physical mechanisms that may lead to the emergence of ruled surfaces on the boundary of the convex set of RDMs. We give an affirmative answer in this work and show that ruled surfaces can also be a consequence of gapless systems. The underlying idea is simple: if the Hamiltonian $H(\vec{\lambda})$ is gapless for some continuous region of the parameter $\vec{\lambda}$, then for each $\vec{\lambda}$, the corresponding low energy states may be projected onto a line on the bound-

ary of the 3-dimensional surface, and the continuous changes of $\vec{\lambda}$ then result in a ruled surface.

We demonstrate our ideas by studying various models of many-body bosonic systems. The choice of such systems are due to their simplicity to analyze. First of all, due to the exchange symmetry of bosons, the wave function $|\psi^N\rangle$ of the system is symmetric and consequently all the 2-RDMs are in fact the same. We then denote such a 2-RDM by ρ_2^N. Furthermore, due to the quantum de Finetti's theorem, in the large N limit, ρ_2^N has a relatively simple description, which is exactly the set of all separable 2-particle density matrices. For low dimensional single particle Hilbert space, e.g. two-mode bosonic system, this then leads to analytical results to the 3-dimensional projections of the set of all ρ_2^N. This allows us to analyze the ruled surfaces on the boundary and their originality.

We study the two-mode Ising model in detail to show a ruled surface that is a direct consequence of gapless systems. We argue that such kind of ruled surfaces are in fact quite a common phenomenon in bosonic systems, since bosons are 'inclined' to be gapless – for any entangled ground states, two-particle correlation functions cannot decay exponentially with any distance defined, due to the symmetry of the system. To distinguish ruled surfaces originated from gapless systems from those from symmetry-breaking solely through the geometry of RDMs, we propose to use finite system size scaling of the corresponding geometry. We apply this finite size scaling method to the two-mode XY model, to identify a ruled surface as a consequence of gapless systems.

II. BACKGROUND AND NOTATIONS

In this section we recall the quantum finite de Finetti's theorem and its consequences on the RDMs. We start with considering an r-mode bosonic system of N bosons with the single-particle Hilbert space $\mathcal{H}$. For our purpose we assume the dimension of $\mathcal{H}$ is finite. Define the collective spin operators of N spins to be

$$J_x^N = \sum_{i=1}^N S_x^i,\ J_y^N = \sum_{i=1}^N S_y^i,\ J_z^N = \sum_{i=1}^N S_z^i. \tag{1}$$

Here $\vec{S}$ is spin operator for spin-$(r-1)/2$.

We consider Hamiltonians with two-body interaction in terms of J_x^N, J_y^N, J_z^N. More precisely, there is in fact a sequence of Hamiltonians for different system size N, each of which is denoted by H^N. We focus on systems that approach the large system size limit (i.e. $N \to \infty$). The celebrated quantum de Finetti's theorem states the following [18–20]: *For any N-boson wave function $|\Psi_N\rangle$ that lies in the symmetric subspace of $\mathcal{H}^{\otimes N}$, and for any constant integer $k > 0$ that is independent of N, the k-RDM ρ_k of $|\Psi_N\rangle$ is a mixture of product states of the form $|\alpha\rangle^{\otimes k}$, in the $N \to \infty$ limit.*

For a two-body Hamiltonian H^N, the ground state energy is determined by the 2-RDM ρ_2^N (of the N-particle wave function $|\Psi_N\rangle$), i.e.

$$E_0^N = \min_{\rho_2^N} \mathrm{tr}(H^N \rho_2^N). \tag{2}$$

According to the quantum de Finetti's theorem, ρ_2^∞ is separable. The set of all ρ_2^∞ is convex, denoted by Θ_2^∞ with the extreme points $|\alpha\rangle|\alpha\rangle$. Therefore in the large N limit, Eq. (2) equals exactly the Hartree's mean field energy. This fact is independent of the details of the Hamiltonian.

We now consider the Hamiltonians with parameters $\vec{\lambda} = (\lambda_0, \lambda_1, \lambda_2)$, i.e.

$$H^N(\vec{\lambda}) = \sum_{i=0}^2 \lambda_i f_i(N) H_i^N, \tag{3}$$

where each H_i^N denotes single particle or two-body interaction in terms of J_x^N, J_y^N, J_z^N for a system of size N, and $f_i(N)$ is a scaling factor to make energy per particle bounded and meaningful in the large N limit. Explicitly, we choose $f_i(N) = 1$ for single particle terms, and $f_i(N) = \frac{1}{N}$ for two-body interaction terms. The set

$$\Theta_2^N(H^N) = \{(x, y, z) | \rho_2^N \in \Theta_2^N\} \tag{4}$$

is a three-dimensional projection of Θ_2^N, where

$$\begin{aligned} x &= \frac{f_0(N)}{N} \mathrm{tr}\left(\rho_2^N H_0^N\right), \\ y &= \frac{f_1(N)}{N} \mathrm{tr}\left(\rho_2^N H_1^N\right), \\ z &= \frac{f_2(N)}{N} \mathrm{tr}\left(\rho_2^N H_2^N\right). \end{aligned} \tag{5}$$

And $H^N(\vec{\lambda})$ corresponds to the supporting hyperplane of $\Theta_2^N(H^N)$, i.e., a parameter vector $\vec{\lambda}$ gives a normal vector of one supporting hyperplane of $\Theta_2^N(H^N)$. For any $\vec{\alpha} \in \Theta_2^N(H^N)$, $\vec{\alpha} \cdot \vec{\lambda} \geq E_0^N(\vec{\lambda})/N$. We also denote that when $N \to \infty$,

$$\Theta_2^\infty(H^\infty) = \{(\bar{x}, \bar{y}, \bar{z}) | \rho_2^\infty \in \Theta_2^\infty\}, \tag{6}$$

where $(\bar{x}, \bar{y}, \bar{z})$ is the corresponding limit of (x, y, z).

We are interested in the geometry of $\Theta_2^N(H^N)$ and its relation with physical properties of the system $H^N(\vec{\lambda})$, especially those related with quantum phase and phase transition.

III. THE TWO-MODE ISING MODEL

We start to examine the geometry of $\Theta_2^N(H^N)$ for the two-mode Ising model, where we take the spin operators as the spin-1/2 Pauli operators for convenience, e.g. $S_x = X, S_y = Y, S_z = Z$. The Hamiltonian reads

$$H_{\mathrm{Ising}}^N = \frac{J}{N}(J_x^N)^2 + B_z J_z^N + B_x J_x^N, \tag{7}$$

where an extra $B_x J_x^N$ term has been added to explicitly break the Z_2 symmetry in the traditional transverse Ising model

when $B_x \neq 0$. This term is chosen for the reason that it corresponds to the order parameter of the Z_2 symmetry-breaking phase of the transverse Ising model [12].

The corresponding

$$\Theta_2^N(H_{\text{Ising}}^N) = \{(x,y,z)|\rho_2^N \in \Theta_2^N\} \tag{8}$$

is given by

$$\begin{aligned} x &= \frac{1}{N^2}\,\text{tr}\left(\rho_2^N (J_x^N)^2\right) \\ &= \text{tr}\left(\rho_2^N (\frac{1}{N} I + \frac{N-1}{N} X\otimes X)\right), \\ y &= \frac{1}{N}\,\text{tr}\left(\rho_2^N J_z^N\right) = \text{tr}\left(\rho_2^N Z\otimes I\right), \\ z &= \frac{1}{N}\,\text{tr}\left(\rho_2^N J_x^N\right) = \text{tr}\left(\rho_2^N X\otimes I\right). \end{aligned} \tag{9}$$

Here by for any two-body operator M, by $\text{tr}(\rho_2^N M)$ we mean $\langle\Psi_N|M|\Psi_N\rangle$. In other words, since all the 2-RDMs of $|\Psi_N\rangle$ are the same, we simply denote it by ρ_2^N and do not specify which two particles ρ_2^N is acting on. Without confusion we will use this convention throughout the paper.

A. Large N limit

In the large N limit, Eq. (8), (9) is equivalent to

$$\Theta_2^\infty(H_{\text{Ising}}^\infty) = \{(\bar{x},\bar{y},\bar{z})|\rho_2^\infty \in \Theta_2^\infty\}, \tag{10}$$

with

$$\begin{aligned} \bar{x} &= \text{tr}(\rho_2^\infty (X\otimes X)), \\ \bar{y} &= \text{tr}(\rho_2^\infty (Z\otimes I)), \\ \bar{z} &= \text{tr}(\rho_2^\infty (X\otimes I)). \end{aligned} \tag{11}$$

The extreme points of $\Theta_2^\infty(H_{\text{Ising}}^\infty)$ are given by

$$\bar{x} = \bar{z}^2,\ \bar{y}^2 + \bar{z}^2 = 1. \tag{12}$$

The boundary surface of $\Theta_2^\infty(H_{\text{Ising}}^\infty)$ is then given by

$$\bar{x} = \bar{z}^2, \text{for}\ \ \bar{y}^2 + \bar{z}^2 \leq 1, \tag{13}$$

and

$$\bar{x} + \bar{y}^2 = 1, \text{for}\ \ \bar{y}^2 + \bar{z}^2 \leq 1. \tag{14}$$

And the corresponding supporting hyperplanes are

$$\bar{x} + \bar{x}_0 - 2\bar{z}_0\bar{z} = 0, \tag{15}$$

and

$$\bar{x} + \bar{x}_0 + 2\bar{y}_0\bar{y} = 2. \tag{16}$$

We observe that there are two ruled surfaces on the boundary of $\Theta_2^\infty(H_{\text{Ising}}^\infty)$. For any point (x_0,y_0,z_0) living on

$$\bar{x} = \bar{z}^2, \text{for}\ \ \bar{y}^2 + \bar{z}^2 \leq 1,$$

we have part of the line (x_0,y,z_0) living on the surface of $\Theta_2^\infty(H_{\text{Ising}}^\infty)$. These points give one ruled surface. For point (x_0,y_0,z_0) lives on

$$\bar{x} + \bar{y}^2 = 1, \text{for}\ \ \bar{y}^2 + \bar{z}^2 \leq 1,$$

we have part of the line (x_0,y_0,z) living on the surface of $\Theta_2^\infty(H_{\text{Ising}}^\infty)$. These points give the other ruled surface.

We show the convex set $\Theta_2^\infty(H_{\text{Ising}}^\infty)$ in Fig. 1. There are two ruled surfaces: the blue one and the green one. Geometrically, these two surfaces have exactly the same shape. However, their physical origins are very different. The Hamiltonian H_{Ising} is known to have a symmetry-breaking phase for $J=-1, B_x=0, |B_z|<2$, and with $J=1, |B_x|<2$ the system is gapless [21]. Therefore, the green ruled surface is due to symmetry breaking when $J=-1, B_x=0, |B_z|<2$, while the blue ruled surface is due to that the system is gapless when $J=1, |B_x|<2$.

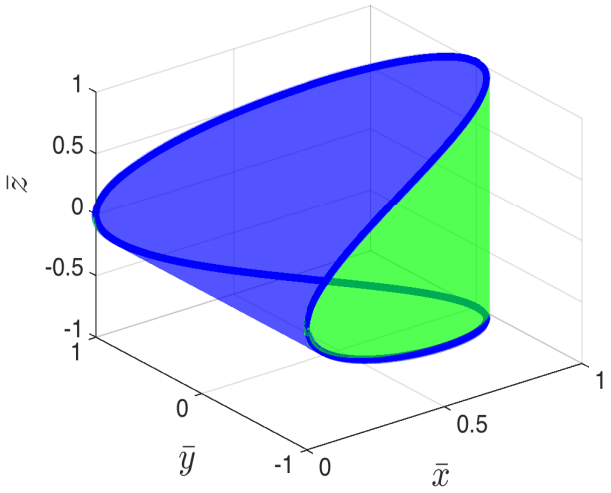


FIG. 1: Convex set for Ising model in the large N limit. It is determined by Eq. (13), (14), with $\bar{x} = \text{tr}(\rho_2^\infty(X\otimes X))$, $\bar{y} = \text{tr}(\rho_2^\infty(Z\otimes I))$, $\bar{z} = \text{tr}(\rho_2^\infty(X\otimes I))$. The green ruled surface is due to symmetry breaking, while the blue ruled surface is due to the fact that the system is gapless in that region.

When $J<0$, for simplicity, we fix $J=-1$. When $B_x=0$, there is a $\mathbb{Z}_2$ symmetry generated by $O = Z_1\otimes Z_2\otimes ...\otimes Z_N$. In the range $B_z\in[-2,2]$, the ground state is two fold degenerate (can be seen from the energy), and a corresponding ruled surface emerge. The phase transition here is Ising type, which can then be explained by mean filed theory (i.e., one only needs to consider separable states, as given in the the calculation of $\Theta_2^\infty(H_{\text{Ising}}^\infty)$).

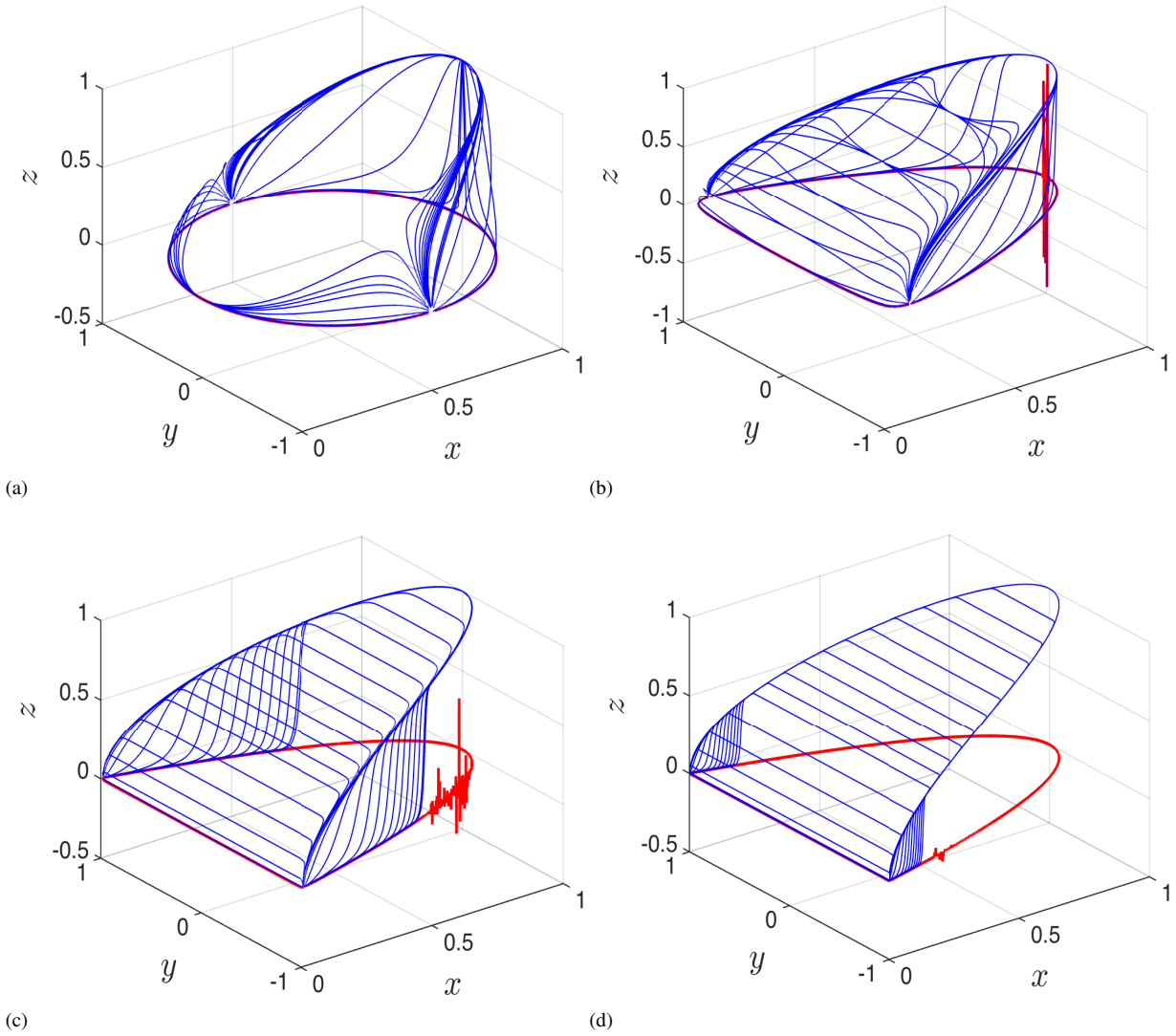


FIG. 2: Convex set $\Theta_2^N(H_{\text{Ising}}^N)$ for two-mode Ising case, with $x = \text{tr}\left(\rho_2^N(\frac{1}{N}I + \frac{N-1}{N}X \otimes X)\right)$, $y = \text{tr}\left(\rho_2^N Z \otimes I\right)$, $z = \text{tr}\left(\rho_2^N X \otimes I\right)$. For clarity, we only show $B_x \leq 0$ part. The result is obtained by exact diagonalization but with different particle numbers. The particle number is $N = 2, 10, 10^2, 10^3$ for (a), (b), (c), (d) respectively. The ruled surface becomes more and more clear with increasing system size.

B. Finite size scaling

Although the two ruled surfaces have exactly the same shape for $N \to \infty$, their different physical origins can be seen from the finite size scaling. The finite N scaling is shown in Fig. 2. Clearly, when N becomes larger, the convex set will go to the $N \to \infty$ limit which is shown in Fig. 1. Due to symmetry we only show the upper part.

Equation (12) can also be verified by the large N data. We remark that, in Fig. 2, there are some special points in the $\Theta_2^N(H_{\text{Ising}}^N)$ for finite N. For example the point with parameter $J = 1, B_x = -1, B_z = 0$. This point seems to be discontinuous from its neighbor. These special points will become normal in the $N \to \infty$ limit.

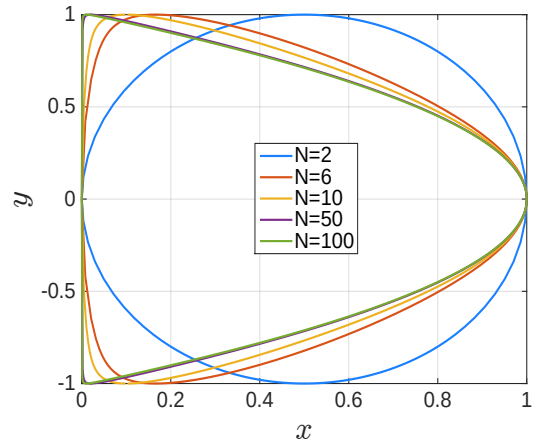
The different origins of the two ruled surfaces can also be viewed from the two-dimensional projections of $\Theta_2^N(H_{\text{Ising}}^N)$, as shown in Fig. 3. In Fig. 3(a), the projection is onto to the xy plane, which corresponds to the Hamiltonian of $B_x = 0$ in H_{Ising}^N. For $B_z = 0$, the Hamiltonian becomes

$$H_{\text{Ising}}^N = \frac{J}{N}(J_x^N)^2, \tag{17}$$

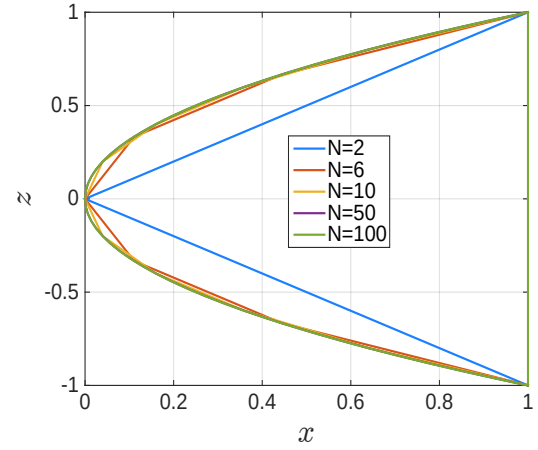
where is a constant that is independent of system size N. The spectra of H_{Ising}^N is then given by

$$E_k^N = \frac{J}{N}k^2, \ k = 0, \pm 2, \pm 4, \ldots, \pm N. \tag{18}$$

When $J > 0$ (corresponding to the blue ruled surface), the ground state corresponding to $k = 0$ is unique, and the spectra



(a)



(b)

FIG. 3: 2D projection of the two-mode Ising convex set $\Theta_2^N(H^N_{\text{Ising}})$. $x = \text{tr}\left(\rho_2^N(\frac{1}{N}I + \frac{N-1}{N}X \otimes X)\right)$, $y = \text{tr}\left(\rho_2^N Z \otimes I\right)$, $z = \text{tr}\left(\rho_2^N X \otimes I\right)$. (a) Projection on to the xy plane. (b) Projection on to the xz plane.

is gapless for $N \to \infty$. When $J < 0$ (corresponding to the green ruled surface), the ground state corresponding to $k = \pm N$ is doubly degenerate, and the spectra has a constant gap.

For any N with $J > 0$, the ground state of $\frac{J}{N}(J_x^N)^2$ is unique which is given by the eigenstate of J_x^N with eigenvalue 0 (denoted by $|J_x = 0\rangle$). This can be seen from the fact the line $x = 0$ only intersects the $2D$ projection of $\Theta_2^N(H^N_{\text{Ising}})$ at the point $(0, 0)$.

However, when $N \to \infty$, the eigenstates of J_z^N with the eigenvalue $\pm N$ (denoted by $|J_z = \pm N\rangle$) will have the same energy per particle as that of $|J_x = 0\rangle$. As a result, in the $N \to \infty$, the line $x = 0$ will intersect the convex set $\Theta_2^\infty(H^\infty_{\text{Ising}})$ at an line interval with end points $(0, 1)$ (corresponding to $|J_z = N\rangle$) and $(0, -1)$ (corresponding to $|J_z = -N\rangle$). The behaviour of the curves approaching the line interval for $x = 0$ when N increases clearly indicates a gapless system (hence the origin of the blue ruled surface), together with a first order phase transition at $B_z = 0$ in the $N \to \infty$ limit.

A similar phenomenon can be observed for all the other line segments on the blue ruled surface. For $J > 0$,$B_x \neq 0$ and $B_z = 0$, the Hamiltonian becomes

$$H^N_{\text{Ising}} = \frac{J}{N}(J_x^N)^2 + B_x J_x^N = \frac{J}{N}\left(J_x^N + \frac{NB_x}{2J}\right)^2 - \frac{NB_x^2}{4J}. \quad (19)$$

The spectra of H^N_{Ising} is then given by

$$E_k^N = \frac{J}{N}\left(k + \frac{NB_x}{2J}\right)^2 - \frac{NB_x^2}{4J},\ k = 0, \pm 2, \pm 4, \ldots, \pm N \quad (20)$$

which is also gapless for $N \to \infty$.

In Fig. 3(b), the projection is onto to the xz plane, which corresponds to the Hamiltonian of $B_z = 0$ in H^N_{Ising}. For $J < 0, B_x = 0$, the ground state is two fold degenerate that are given by $|J_x = \pm N\rangle$, which is even exact for finite N. The system has a $\mathbb{Z}_2$ symmetry, and the symmetry-breaking ground states are $|J_x = \pm N\rangle$. This indicates that the green ruled surface is due to symmetry-breaking.

Before we end this section, we would like to remark that, the stability of the points in the convex set is not the same for all points. The points on the ruled surfaces with gapless systems are more fragile than others, in the sense they only occur in a relatively narrow parameter region and will leave that area under a small parameter change. Points on the symmetry breaking ruled surface are more stable. Also, there is some 'even-odd effect' for this model, i.e., for even particle number and odd particle number, the result may have some difference. But this difference is not important here, and in both cases the limit will be the same $\Theta_2^\infty(H^\infty_{\text{Ising}})$. For simplicity we only show the N even case.

IV. GAPLESS SYSTEMS AND RULED SURFACES

As discussed in Sec. III, ruled surfaces on the boundary of $\Theta_2^\infty(H^\infty)$ may be a result of either symmetry-breaking or gapless systems. If we know the gap/symmetry properties of the system, then we can tell the physical origin of each ruled surface. However, suppose we have no such knowledge of the system and hope to learn something solely from the geometry, then there is no way to tell such a difference (e.g. the blue and green ruled surfaces in Fig. 1 have exactly the same geometric shape).

In order to tell the difference, we will then need to use finite size scaling of $\Theta_2^N(H^N)$. By computing boundary lines corresponding to ground states of H^N, shown in Fig. 3, symmetry-breaking systems show very different behaviors comparing to gapless systems. We will hence propose to use finite size scaling to study the origin of ruled surfaces in $\Theta_2^\infty(H^\infty)$, and use the following system as an example for applying our idea of finite size scaling.

Consider the two-mode XY model, where $S_x = X, S_y = Y, S_z = Z$ are Pauli operators for qubit. The Hamiltonian

reads

$$H_{\rm XY}^N = \frac{1}{N}\left(J_1(J_x^N)^2 + J_2(J_y^N)^2\right) + B_z J_z^N. \tag{21}$$

The corresponding $\Theta_2^N(H_{\rm XY}^N)$ is generated by

$$\begin{aligned} x &= \frac{1}{N^2}\,\mathrm{tr}\left(\rho_2^N (J_x^N)^2\right) \\ &= \mathrm{tr}\left(\rho_2^N (\frac{1}{N} I + \frac{N-1}{N} X\otimes X)\right), \\ y &= \frac{1}{N^2}\,\mathrm{tr}\left(\rho_2^N (J_y^N)^2\right) \\ &= \mathrm{tr}\left(\rho_2^N (\frac{1}{N} I + \frac{N-1}{N} Y\otimes Y)\right), \\ z &= \frac{1}{N}\,\mathrm{tr}\left(\rho_2^N J_z^N\right) = \mathrm{tr}\left(\rho_2^N Z\otimes I\right). \end{aligned}$$

for $\rho_2^N \in \Theta_2^N(H_{\rm XY}^N)$. In the $N\to\infty$ limit, this is equivalent to

$$\begin{aligned} \Theta_2^\infty(H_{\rm XY}^\infty) =& \{\mathrm{tr}(\rho_2^\infty(X\otimes X)), \mathrm{tr}(\rho_2^\infty(Y\otimes Y)), \\ & \mathrm{tr}(\rho_2^\infty Z\otimes I))|\rho_2^\infty \in \Theta_2^\infty\}. \end{aligned} \tag{22}$$

Let

$$\begin{aligned} \bar{x} &= \mathrm{tr}(\rho_2^\infty(X\otimes X)), \\ \bar{y} &= \mathrm{tr}(\rho_2^\infty(Y\otimes Y)), \\ \bar{z} &= \mathrm{tr}(\rho_2^\infty(Z\otimes I)), \end{aligned} \tag{23}$$

the extreme points of $\Theta_2^\infty(H_{\rm XY}^\infty)$ satisfy

$$\bar{x} + \bar{y} + \bar{z}^2 = 1,\ \bar{x}\geq 0,\ \bar{y}\geq 0. \tag{24}$$

This is also the boundary surface of $\Theta_2^\infty(H_{\rm XY}^\infty)$. The corresponding supporting hyperplanes are

$$\bar{x} + \bar{x}_0 + \bar{y} + \bar{y}_0 + 2\bar{z}_0\bar{z} = 2,\ \bar{x}\geq 0,\ \bar{y}\geq 0. \tag{25}$$

We show the convex set $\Theta_2^\infty(H_{\rm XY}^\infty)$ in Fig. 4. There is a blued ruled surface on the boundary, together with two plane areas given by the intersection of $\Theta_2^\infty(H_{\rm XY}^\infty)$ with the planes $\bar{x}=0$ and $\bar{y}=0$ respectively. For any point (x_0, y_0, z_0) living on the surface

$$\bar{x} + \bar{y} + \bar{z}^2 = 1,\ \bar{x}\geq 0,\ \bar{y}\geq 0,$$

part of the line $(x, 1-x-z_0^2, z_0)$ also lives on this surface.

While the two planes corresponds to gapless systems, the question is what is the origin of the blued ruled surfaces, i.e., whether it results from symmetry-breaking or gapless systems. To learn more information, we will then need the finite size scaling behaviors of $\Theta_2^N(H_{\rm XY}^N)$, which we show in Fig. 5.

We also show the $2D$ projection of $\Theta_2^N(H_{\rm XY}^N)$ onto the xy plane in Fig. 6. This corresponds to $B_z = 0$, and the Hamiltonian becomes

$$H_{\rm XY}^N = \frac{1}{N}\left(J_1(J_x^N)^2 + J_2(J_y^N)^2\right). \tag{26}$$

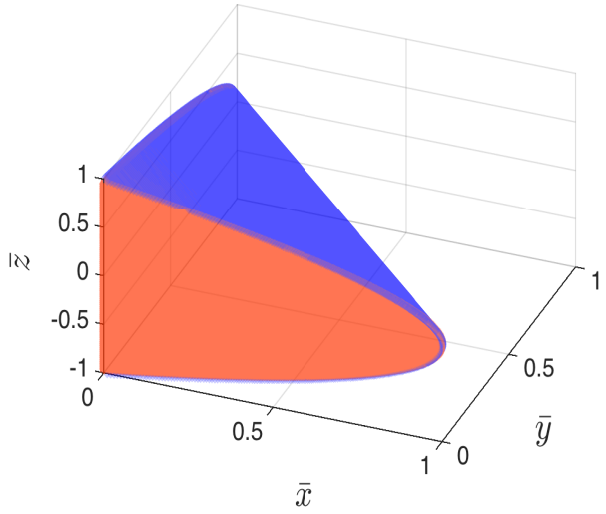


FIG. 4: Convex set for two-mode XY model in the large N limit. It is determined by equation (24), with $\bar{x} = \mathrm{tr}(\rho_2^\infty(X\otimes X))$, $\bar{y} = \mathrm{tr}(\rho_2^\infty(Y\otimes Y))$, $\bar{z} = \mathrm{tr}(\rho_2^\infty(Z\otimes I))$. The convex set is symmetric with respect to interchange of $\bar{x}$ and $\bar{y}$ axis.

For $J_1 = J_2$, we have

$$\begin{aligned} H_{\rm XY}^N &= \frac{1}{N}\left(J_1(J_x^N)^2 + J_2(J_y^N)^2\right) \\ &= \frac{J_1}{N}((J^N)^2 - (J_z^N)^2), \end{aligned} \tag{27}$$

where the operator $(J^N)^2 = (J_x^N)^2 + (J_y^N)^2 + (J_z^N)^2$. The spectra of $H_{\rm XY}^N$ is then given by

$$E_k^N = \frac{J_1}{N}\left(N(N+2) - k^2\right),\ k = 0, \pm 2, \pm 4, \ldots, \pm N, \tag{28}$$

which is gapless for $N\to\infty$ when $J_1 < 0$ (corresponding to the blue ruled surface).

The projection of $\Theta_2^\infty(H_{\rm XY}^\infty)$ is in fact a triangle with vertices $(0,0), (1,0), (0,1)$. The finite size scaling of $\Theta_2^N(H_{\rm XY}^N)$ clearly approaches each boundary line of this triangle in the $N\to\infty$ limit, indicating gapless systems. That is, the blue ruled surface results from gapless systems. There is in fact no ruled surface resulting from symmetry-breaking in the geometry of $\Theta_2^N(H_{\rm XY}^N)$.

V. DISCUSSION

In this work, we have examined the geometry of reduced density matrices for bosonic systems, which are convex sets in $\mathbb{R}^3$. Our focus is on the physical origin of the ruled surfaces on the boundary of these convex sets. We show that apart from signatures of symmetry-breaking, ruled surfaces can also be a consequence of gapless systems. Concrete examples are examined for bosonic system in the $N\to\infty$ limit, and ruled surfaces due to gapless systems are shown. Thanks

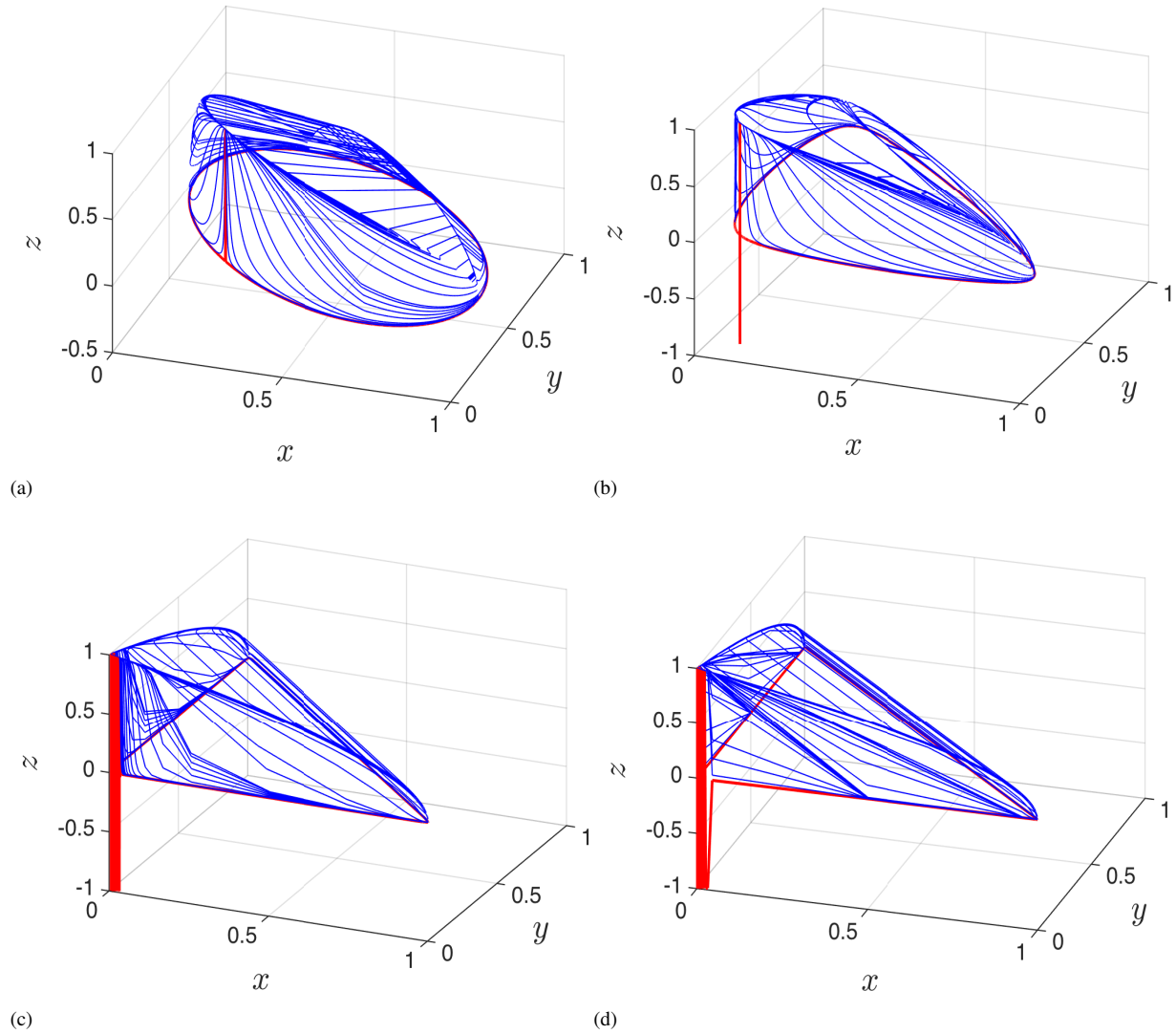


FIG. 5: Convex set $\Theta_2^\infty(H_{\rm XY}^\infty)$ for two-mode XY model with finite system size N, where $x = \mathrm{tr}\left(\rho_2^N(\frac{1}{N}I + \frac{N-1}{N}X\otimes X)\right)$, $y = \mathrm{tr}\left(\rho_2^N(\frac{1}{N}I + \frac{N-1}{N}Y\otimes Y)\right)$, $z = \mathrm{tr}\left(\rho_2^N Z\otimes I\right)$. System size is $N = 4, 10, 2\times 10^2, 10^3$, for (a),(b),(c),(d). For simplicity, we only show $B_z \le 0$ part.

to the quantum de Finetti's theorem, the geometry of the reduced density matrices of the discussed bosonic models can be found analytically.

In more general cases where there is no longer bosonic exchange symmetry, we would expect that the relationship between gapless systems and the emergence of ruled surface on the boundary of three-dimensional projections of reduced density matrices will remain valid, since the bosonic exchange symmetry is not essential for having those ruled surfaces. For general systems without bosonic exchange symmetry, however, quantum de Finetti's theorem is no longer valid, and the geometry of 2-RDMs is hard to get in general [6–8]. Nevertheless, it is interesting to study other concrete systems whose geometry of 2-RDMs will also have ruled surface on the boundary that is related to gapless systems. We leave this for future work.

ACKNOWLEDGEMENT

We thank Yi Shen and Li You for helpful discussions. B.Z. is supported by NSERC and CIFAR. X.Q. is supported by program for the Outstanding Innovative Teams of Higher Learning Institutions of Shanxi. This research was supported in part by Perimeter Institute for Theoretical Physics. Research at Perimeter Institute is supported by the Government of Canada through Industry Canada and by the Province of Ontario through the Ministry of Economic Development & Innovation.

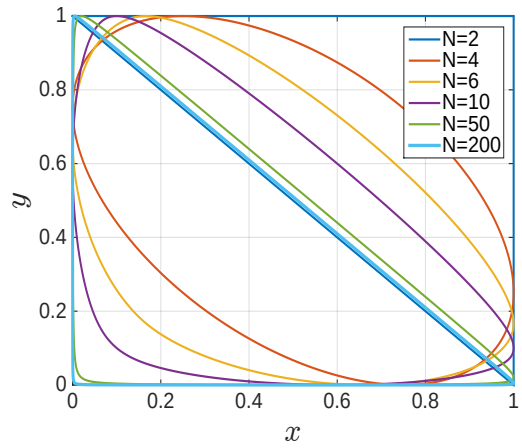


FIG. 6: 2D projection of $\Theta_2^N(H_{\rm XY}^N)$ onto the xy plane, where $x = \mathrm{tr}\left(\rho_2^N(\frac{1}{N}I + \frac{N-1}{N}X\otimes X)\right)$, $y = \mathrm{tr}\left(\rho_2^N(\frac{1}{N}I + \frac{N-1}{N}Y\otimes Y)\right)$.

[1] A. J. Coleman, Rev. Mod. Phys. **35**, 668 (1963).
[2] R. M. Erdahl, Journal of Mathematical Physics **13**, 1608 (1972).
[3] A. A. Klyachko, in *Journal of Physics: Conference Series*, Vol. 36 (IOP Publishing, 2006) p. 72.
[4] R. Erdahl and B. Jin, in *Many-Electron Densities and Reduced Density Matrices*, Mathematical and Computational Chemistry, edited by J. Cioslowski (Springer US, 2000) pp. 57–84.
[5] C. A. Schwerdtfeger and D. A. Mazziotti, The Journal of Chemical Physics **130**, 224102 (2009).
[6] Y.-K. Liu, in *Approximation, Randomization, and Combinatorial Optimization. Algorithms and Techniques*, Lecture Notes in Computer Science, Vol. 4110, edited by J. Diaz, K. Jansen, J. D. Rolim, and U. Zwick (Springer Berlin Heidelberg, 2006) pp. 438–449.
[7] Y.-K. Liu, M. Christandl, and F. Verstraete, Phys. Rev. Lett. **98**, 110503 (2007).
[8] T.-C. Wei, M. Mosca, and A. Nayak, Phys. Rev. Lett. **104**, 040501 (2010).
[9] F. Verstraete and J. I. Cirac, Phys. Rev. B **73**, 094423 (2006).
[10] G. Gidofalvi and D. A. Mazziotti, Phys. Rev. A **74**, 012501 (2006).
[11] J. Chen, Z. Ji, C.-K. Li, Y.-T. Poon, Y. Shen, N. Yu, B. Zeng, and D. Zhou, New Journal of Physics **17**, 083019 (2015).
[12] V. Zauner, L. Vanderstraeten, D. Draxler, Y. Lee, and F. Verstraete, arXiv preprint arXiv:1412.7642 (2014).
[13] J.-Y. Chen, Z. Ji, Z.-X. Liu, Y. Shen, and B. Zeng, Physical Review A **93**, 012309 (2016).
[14] J. W. Gibbs, Transcations of the Connecticut Academy **2**, 309 (1873).
[15] J. W. Gibbs, Transcations of the Connecticut Academy **2**, 382 (1873).
[16] J. W. Gibbs, Transcations of the Connecticut Academy **3**, 108 (1875).
[17] R. B. Israel, *Convexity in the Theory of Lattice Gases* (Princeton University Press, 1979).
[18] E. Størmer, Journal of Functional Analysis **3**, 48 (1969).
[19] R. L. Hudson and G. R. Moody, Probability Theory and Related Fields **33**, 343 (1976).
[20] M. Lewin, P. T. Nam, and N. Rougerie, Advances in Mathematics **254**, 570 (2014).
[21] A. J. Leggett, Reviews of Modern Physics **73**, 307 (2001).